Analysis on Evolution of the Energy Contribution for Coherent Structure in Cylindrical Near-wake Flow Using Proper Orthogonal Decomposition

Tzu-Hsun Lin and Keh-Chin Chang*
Department of Aeronautics and Astronautics, National Cheng Kung University, Taiwan
* Corresponding author, e-mail: kcchang@ncku.edu.tw

Abstract

Evolution of the energy contribution for coherent structure in the near wake behind a circular wake are studied using POD analysis with the PIV data at two Reynolds numbers of 3840 and 9440 which are of subcritical wake regime. Identification of coherent structure in the wake is carried out by checking the Fourier power spectrum of each temporal mode coefficient and selecting those with their peak magnitudes greater than the smallest magnitude of the identified harmonic-frequency family (if existed) as the large-scale organized motions. The energy contributed by coherent structure is estimated from the integral of all the peak impulses over the frequency domain. It shows that energy percentage contributed by coherent structure is significantly dependent on Re and its streamwise location in near wake. The evolution of the energy percentage contributed by coherent structure exhibits monotonically a decaying trend as moving downstream. Constitution of coherent structure is also examined.

Keywords: *Turbulent near wake, Coherent structure, POD*

1. Introduction

Turbulent flows behind a bluff body are complex multi-scale and chaotic motions that are referred to coherent turbulent structures involving coherent vortices (in other words, large-scale organized motions) and small-scale fluctuating motions. The organized motions in a coherent structure are classified with the K*á*rm*á*n vortices, which are the principal motions, and the secondary vortices [1, 2]. The secondary vortices consist of longitudinal smaller-scale vortices originated from parts of the spanwise vortices [3] and Kelvin-Helmholtz vortices originated from the velocity shear layer and characterized with high frequencies than the natural frequency of K*á*rm*á*n vortex formation [4]. The kinematic properties of these motions such as vorticity, variances of velocity components and energy govern the way coherent structures grow, evolve and decay. Almost all existing studies on these topics were in terms of the properties of vorticity and variances of velocity components rather than the property of energy of the coherent turbulent structures. This is because an exact assessment of the ratio of kinetic energy contributed by coherent structure is practically impossible in view of the experimental difficulties [5]. However, an estimate of around 25% to this ratio for near wake was reported in a review paper of Fieldler [5].

The proper orthogonal decomposition (POD) is a common method to extract the essential features from a snapshot sequence of flow fields from experimental measurements or numerical simulations. Advances on the detecting capability in both spatial and temporal resolutions for the particle image velocimetry (PIV) lead to a situation that the measured information for the spatially phase-correlated vorticity can be used to study the dynamic of a coherent structure [6, 7]. POD decomposes a large-quantity data set into spatial eigenmodes and temporal coefficients that correspond to each eigenmode [8, 9]. The eigenvalue for each eigenmode represents physically the contribution of the kinetic energy of the basis, that is, the total kinetic energy of the flow. Eigenmodes are then ordered by their magnitudes of the eigenvalues as $\lambda_\ell > \lambda_{\ell+1}$ so that the first mode corresponds to the most energetic component of the data set.

This study uses the approach developed recently by Chu and Chang [10] to identify the coherent structure and simultaneously estimate the energy contribution for each multi-dominant large-scale, organized component using velocity data that are measured by PIV in a turbulent near-wake flow field behind a long circular cylinder. Evolution of the coherent structure in the near-wake is shown by observing the variation of the energy contribution along the streamwise (main flow stream) direction.

2. Experimental and Analysis Methods

2.1 Experimental details

Experiments are conducted in a vertically downward, rectangular wind tunnel with the freestream velocities of 5.97 m/s and 14.67 m/s, which are respectively equivalent to Reynolds numbers (based on the diameter of the circular cylinder, d) of 3860 and 9440 and are hereafter named as Cases 1 and 2, respectively. These two cases are in the subcritical wake regime ($Re = 10^3 - 2 \times 10^5$) with St ≈ 0.21 [11]. The Strouhal number is defined by

$$St = (f \times d)/u_{ref} \quad (1)$$

where f and u_{ref} are the Kármán vortex shedding frequency and the upstream free-stream velocity, respectively. The test section has a cross sectional area of 150 mm × 150 mm and a length of 600 mm. A circular cylinder diameter of 10 mm, acting a wake generator, is mounted in the middle of the cross section, 75 mm down from the top of the test section. The streamwise (x) and transverse (y) coordinates are positive downward and positive toward the right, respectively. The origin is set at the cylinder's centre. The inlet turbulent intensity measured at x = − 70 mm is about 1%. The measured domain is 155 mm × 100 mm (x by y) in the central plane of the test section.

A two-component PIV system is used for velocity measurement. The frame rate is 10^4 frame/s with a spatial resolution of 1024 pixels by 1024 pixels. The uncertainty of the PIV measurement is estimated about 3.1%. A total of 43,683 PIV image pairs are collected in the experiment. More information for the employed PIV system and its operational conditions is referred to our previous studies [10, 12] and is not repeated here.

2.2 POD analysis

The snapshot POD method [8], discretizing time rather than space which fits the present study due to a situation of the number of snapshots in time far exceeding the number of spatial points [12], is used to decompose the two-dimensional temporal flow field at instant time t_ℓ in terms of the triple decomposition as

$$u_i(x,y,t_\ell) = \bar{u}_i(x,y) + \tilde{u}_i(x,y,t_\ell) + u_i''(x,y,t_\ell) = \bar{u}_i(x,y) + \sum_{n=1}^{N} a_{i,n}(t_\ell)\phi_{i,n}(x,y) \quad (2)$$

where $\bar{u}_i, \tilde{u}_i, u_i''$ are respectively a component of mean, organized and randomly fluctuating motion; $\phi_{i,n}$'s and $a_{i,n}'s$ are respectively the spatial eigenmodes and the temporal mode coefficients. The upper bound of the series, N, should be the same as the total collected PIV image pairs in the experiment, that is, 43,683. However, judging with the accuracy (3.1%) for the employed PIV measurements, the N values of 25,000 and 30,000, which are sufficient to attain statistically stationary results for the POD analyses of Cases 1 and 2, respectively [12], are set in the study. Figure 1 shows two power spectra of the stream-wise velocity measured respectively at the locations (x/d = 2, y/d = 0.55) for Case 1 and (2, 0.57) for Case 2, where are around the wake width, defined by $u/u_\infty = 0.95$ where u_∞ is the freestream velocity, for each case. The Kármán vortex shedding (or first harmonic) frequencies are 126 Hz and 305 Hz for Cases 1 and 2, respectively, (see Fig. 1) which lead

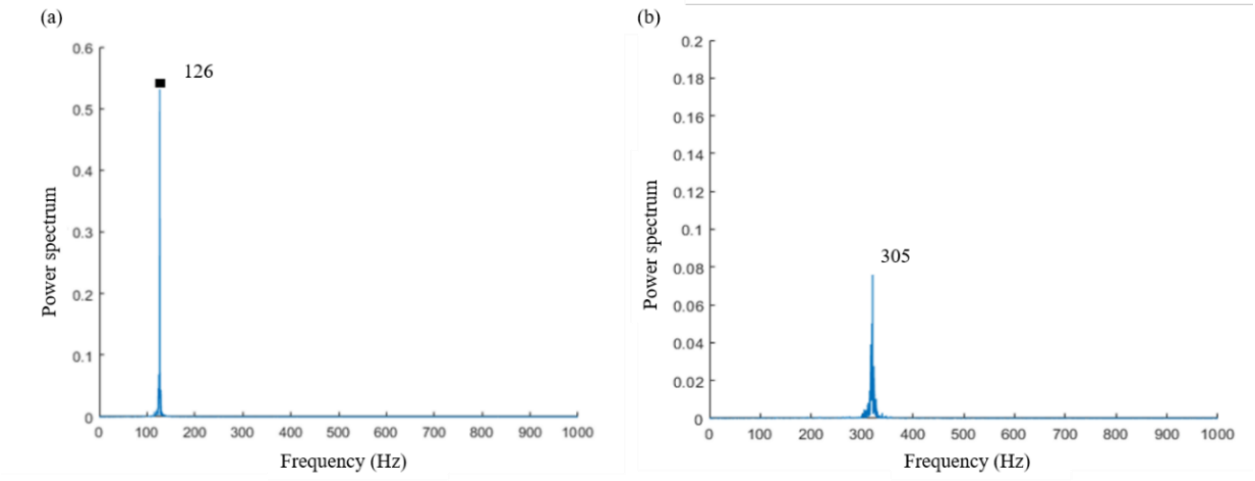

Fig.1 Fourier power spectra of the stream-wise velocity for Case 1 at location ($^{x}/_{d} = 2$, $^{y}/_{d} = 0.55$) and for Case 2 at location (2, 0.57)

to St values respectively equal to 0.211 and 0.208. The field of view (FOV) should be capable of catching the maximum spacing (λ) of vortices in the K*á*rm*á*n vortex street and is estimated with the relationship of $\lambda = d/St$. Thus, the λ values should be larger than 4.74d and 4.81d for Cases 1 and 2, respectively. FOV is set to be 5 d in the following POD analysis. More information for POD analysis is referred to our previous studies [12] and is not repeated here

3. Results and Discussion

Identification of coherent structure, that is, large-scale organized motions, for each eigenmode of Eq. (2) follows the approach developed by Chiu and Chang [10] and is briefly outlined in the following. As reported in our previous studies [10, 12] for the Fourier spectrum analysis on each mode coefficient for both investigated cases, there exist at most three (1st, 2nd and 3rd) harmonic frequencies in the integral-scale subrange of the frequency domain, while the higher harmonic frequencies are located beyond the inertia subrange (in other words, Taylor microscale which is classified as the randomly fluctuating component in Eq. (2)) of frequency domain. These three large-scale harmonic frequencies (126, 252 and 378 Hz for Case 1 as well as 305, 610 and 915 Hz for Case 2) are respectively referred to the harmonic-frequency families hereafter for Cases 1 and 2. In view of the members of harmonic-frequency family being large-scale organized motions in the K*á*rm*á*n vortex street, the peak frequencies for which the magnitudes are larger than the smallest magnitude of the harmonic-frequency family in the Fourier power spectrum are taken as the large-scale organized motions [6, 10] for each eigenmode. The non-harmonic peak frequencies are the secondary vortices.

Three streamwise subranges (each with the size of one FOV) is, 0.5d – 5.5d, 5.5d – 10.5d and 10.5d – 15.5d for each case, are analysed to investigate evolution of the energy contribution for coherent structure in the near wake. Table 1 presents the percentages of kinetic energy on the entire eigenmodes contributed by the first 25 modes in the streamwise subrange of 5.5d – 10.5d for Case 2 as an example to demonstrate how to estimate the percentages of kinetic energy contributed respectively by the coherent structure and by the harmonic-frequency family. The cumulative kinetic energy for the first 25 modes reaches slightly over 80% total kinetin energy of entire eigenmodes. Note that the kinetic energy contributed by the 25th mode is as low as around 0.5% total kinetic energy and the values for the further increasing modes monotonously collapse to a negligible level.

Based on the specified coherent-structure identification process for the temporal coefficients of the 1st and 2nd modes, there is only one frequency at 305 Hz in the domain of interest which contributes respectively 1.688% and 1.170% total kinetic energy for each mode, respectively (see Table 1). Such feature, possessing only one peak (1st harmonic) frequency and with similar levels of kinetic energy, is observed at least for the two first modes in the POD analyses for all three investigated streamwise subregions of each case. There are no dominant frequencies in each power spectrum of the temporal coefficient for the next three (3rd, 4th and 5th) modes, but multiple dominant frequencies are observed in the power spectra of the temporal coefficients in the 6th to 17th modes. For example, the 1st and 2nd harmonic frequencies and some non-harmonic frequencies, which are classified as the secondary vortices, are observed in the 6th mode (see Table 1), but the most dominant vortex is a non-harmonic one (i.e., secondary vortex). As shown in Table 1, this situation also occurs in the 7th to 17th modes. Nevertheless, the most dominant vortices in the 21st and 22nd modes are the first harmonic frequency. The integral of all peak impulses, which are identified as large-scale organized motions, over the frequency domain for the 6th mode gives a value of 0.1256% denoting the percentage of the kinetic energy contributed by the coherent structure at this mode (see Table 1). Similarly, an integral of the peak impulses but is limited to members of the harmonic-frequency family over the frequency domain for the 6th mode gives a value of 0.005506% denoting the percentage of the kinetic energy contributed by the harmonica-frequency family (see Table 1). After performing all analysis procedures for the first 25 modes and recording the results in Table 1, the sums for the kinetic energy contributed respectively by the coherent structure and the harmonic-frequency family are 3.686% and 3.338%. It shows that the harmonic-frequency family contributes 3.338%/3.686% = 90.5% kinetic energy of the coherent structure and the remainder is contributed by the secondary vortices. Following the same analysis approach, the sums of the kinetic energy contributed respectively by the coherent structure and the harmonic-frequency family are calculated for the other subregions (0.5d -5.5d and 10.5d – 15.5d) of Case 2 and all three subregions of Case 1 and are summarized in Tables 2 and 3. The detailed information of these analyses is referred to Lin [13].

Table 1 Identification of the large-scale motions and the kinetic-energy percentages contributed by the large-scale motions and the harmonic-frequency vortices for the first 25 modes in the flow subrange of 5.5 d – 10.5 d for Case 2.

Mode	Dominant frequencies (Hz)	% of kinetic energy				
		On entire eigenmodes	contributed by			
			Organized-motion parts on each mode	Organized-motion parts on entire eigenmodes	Harmonic-frequency parts on all organized-motion parts	Harmonic-frequency parts on entire eigenmodes
1	1st harmonic	1.948 E+01	8.666 E+00	1.688 E+00	1.000 E+02	1.688 E+00
2		1.429 E+01	8.192 E+00	1.700 E+00	1.000 E+02	1.170 E+00
3	none	8.938 E+00				
4		8.640 E+00				
5		5.506 E+00				
6	P*: nonharmonic O*: including 1st and 2nd harmonics	3.378 E+00	3.718 E+00	1.256 E−01	4.384 E+00	5.506 E−03
7	P: nonharmonic O: including 1st harmonic	2.641 E+00	4.288 E+00	1.132 E−01	2.541 E+00	2.877 E−03
8		1.764 E+00	4.753 E+00	8.384 E−02	2.629 E+00	2.204 E−03
9		1.674 E+00	1.124 E+00	1.882 E−02	2.856 E+01	5.374 E−03
10	P: nonharmonic O: including 1st, 2nd and 3rd harmonics	1.414 E+00	3.146 E+00	4.449 E−02	1.322 E+01	5.883 E−03
11		1.334 E+00	2.070 E+00	2.763 E−02	2.057 E+01	5.682 E−03
12		1.316 E+00	2.216 E+00	2.915 E−02	1.133 E+01	3.302 E−03
13	P: nonharmonic O: including 1st harmonic	1.161 E+00	3.280 E+00	3.809 E−02	7.073 E+00	2.694 E−03
14		1.068 E+00	2.964 E+00	3.164 E−02	4.453 E+00	1.409 E−03
15		9.557 E−01	2.240 E+00	2.141 E−02	3.438 E+00	7.359 E−04
16	P: nonharmonic O: including 1st and 2nd harmonics	9.415 E−01	2.965 E+00	2.792 E−02	1.377 E+01	3.843 E−03
17		8.169 E−01	2.734 E+00	2.233 E−02	1.010 E+00	2.255 E−04
18	none	7.645 E−01				
19		7.244 E−01				
20		6.935 E−01				
21	P: 1st harmonic O: including 2nd harmonic	6.592 E−01	1.488 E+00	9.808 E−03	4.402 E+01	4.317 E−03
22	P: nonharmonic O: including 1st harmonic	6.487 E−01	1.027 E+00	6.663 E−03	1.782 E+01	1.187 E−03
23	P: 1st harmonic O: including 2nd harmonic	5.794 E−01	1.395 E+00	8.028 E−03	3.419 E+01	2.763 E−03
24	none	5.587 E−01				
25		5.427 E−01				
sum		8.049 E+01		3.686 E+00		3.338 E+00

* P: primary, O: others

In contrast to the estimate of ~ 25% energy contribution by coherent structure in near wake reported in an early review paper [5] but without giving information regarding Re, location in the flow and the estimation approach, Table 2 shows that energy contribution ratio by coherent structure is significantly dependent on Re and its streamwise subregion in the near wake. According to the study of Dynnikova et al. [14], the K*árm*án vortex street decays until the transformation into a secondary vortex street of low frequency and stronger vortices in the far wake. The streamwise evolutions of the contribution percentages of the kinetic energy by coherent structure for two cases in Table 2 do meet this trend. There are large changes in the contribution percentages of the kinetic energy by coherent structure as Re number is increased from 3840 (Case 1) to 9440 (Case 2). It can be attributed to a fact that the turbulence level, contributed by the fluctuating motions, u_i'', in

Eq. (2), is enhanced with increasing Re value and thus reduce the weight of the energy contributed by coherent structure in the near wake, i.e., $\tilde{u}_i$, in Eq, (2), as shown for Case 2. Yiu et al. [15] studied the Reynold number (varying from 10^3 *to* 10^4) effects on three-dimensional vorticity in turbulent near wake. They found a large jump of turbulent dynamics such as streamwise vorticity and vortex formation length from Re = $5\times\ 10^3$ to Re = 10^4. The results shown in Table 2 is consistent with the trend observed by Yiu et al. [15].

Table 2 Streamwise evolution of the percentage of kinetic energy contributed by coherent structure for the two investigated cases

Case	Re	x = 0.5 – 5.5 d	x = 5.5 –10.5 d	x = 10.5 – 15.5 d
1	3840	36.1%	8.51%	4.12%
2	9440	5.84%	3.69%	3.25%

Table 3 Streamwise evolution of the cumulative percentage of kinetic energy contributed by the harmonic-frequency family to that by coherent structure for the two investigated cases

Case	x = 0.5 – 5.5 d	x = 5.5 –10.5 d	x = 10.5 – 15.5 d
1	99.2%	94.3%	84.3%
2	70.0%	90.5%	84.3%

It is known that the longitudinal vortices are superimposed on the K*á*rm*á*n vortices above certain Reynolds numbers (> 140) [16] making three-dimensionalities of coherent structures in a circular-cylinder wake. The experimental study of Huang et al. [17] revealed that the longitudinal vortices appeared in the spanwise (x, z) plane in the immediate proximity behind the cylinder and the vortex formation length shrank with increasing Re for the Re range of $2\times\ 10^3$ to 10^4. It also showed that the longitudinal vortices decayed rapidly from x/d = 5 to 10 and slowly for x/d > 10. The information concluded in the past researches shows that the longitudinal vortices are the primary constituent of the secondary vortex in a very upstream subregion of near wake. Table 3 show evolutions of the cumulative energy percentage contributed by the harmonic-frequency family (i.e., the K*á*rm*á*n vortices) to that contributed by the coherent structure for two investigated cases. For Case1 at Re = 3860, almost all the coherent structure is initially contributed by the K*á*rm*á*n vortices (99.2%) in the immediate proximity behind the cylinder; and the energy contribution of the longitudinal vortices to the coherent structure is gradually enhanced along with the streamwise distance. However, for Case 2 at Re = 9440, energy contribution by the longitudinal vortices to the coherent structure in the immediate proximity behind the cylinder dramatically jumps to ~ 30% but decays rapidly, which is consistent with the observation in the study of Huang et al. [17], to a minor portion (< 10%) in the subregion of x/d = 5.5 – 10.5, and then decays slowly as Case 1 in the downstream subregion of x/d = 10.5 – 15.5. Since the present identification of the large-scale organized motions is performed on basis of harmonic-frequency family, it may argue that the contribution of the secondary vortices could be underestimated. Nevertheless, as checking for the energy contribution in entire eigenmodes in the subregion of x/d = 0.5 – 5.5 for Case 2, the first four modes possess only one peak impulse at the 1st harmonic frequency and their sum for the kinetic energy contribution equal to 32.9% [13], which is equivalent to 32.9%/70% = 47% of 70% shown in Table 3. Such speculation for underestimation of the energy contribution by the secondary vortices would not become a significant issue. However, the estimation of the energy contribution for coherent structure can be definitely improved by an additional identification process for the longitudinal vortices and it remains to be developed.

2. Conclusions

Estimations of the kinetic-energy percentage contributed by coherent structure on the total kinetic energy of entire eigenmodes are performed using POD analysis with the PIV data for three consecutive streamwise one-FOV subregions behind a circular cylinder at two Reynolds numbers. Identification of coherent structure in the flow is carried out by checking the Fourier power spectrum of each temporal mode coefficient and selecting those with their peak magnitudes greater than the smallest magnitude of the identified harmonic-frequency family (if existed) as the large-scale organized motions. The energy contributed by coherent

structure is then estimated from the integral of all these peak impulses over the frequency domain. It shows that energy percentage contributed by coherent structure is significantly dependent on Re and its streamwise location in the near wake. The streamwise evolutions of the energy percentage contributed by coherent structure exhibit monotonically decaying trend as moving downstream for both investigated cases. For the case of Re = 3840 (Case 1), almost all the coherent structure is initially contributed by the K*á*rm*á*n vortices in the immediate proximity behind the cylinder but energy contribution by the secondary vortices is gradually increased along with the streamwise distance. In contrast to Case 1, energy percentage contributed by the secondary vortices, which are mainly from the longitudinal vortices, to the coherent structure in the immediate proximity behind the cylinder for the case of Re = 9440 jumps from < 1% (Case 1) to 30% but decays rapidly to the next streamwise subrange (x/d = 5.5 – 10.5) and slowly for x/d > 10.5, which agrees with the observation of the previous study in literature.

References

[1] Wei T. and Smith C.R., "Secondary vortices in the wake of circular cylinder", *Journal of Fluid Mechanics*, Vol. 169 (1986), pp. 513-533.

[2] Brede M., Eckelmann, H. and Rockwell, D., "On secondary vortices in the cylinder wake", *Physics of Fluids*, Vol. 8, No. 8 (1996), pp. 2117-2124.

[3] Zhang H.J., Zhou Y. and Antonia R.A., "Longitudinal and span-wise vertical structure in a turbulent near wake", *Physics of Fluids*, Vol. 12, No. 11 (2000), pp. 2954-2964.

[4] Chyu C. Lin J.C., Sheridan J. and Rockwell D., "Karman vortex formation from a cylinder: role of phase-locked Kelvin-Helmholtz vortices", *Physics of Fluids*, Vol. 7, No. 9 (1995), pp. 2288-2290.

[5] Fieldler H.E., "Coherent structure in turbulent flow", *Progress in Aerospace Science*, Vol. 25 (1988), pp. 231-269.

[6] Zhang Q., Liu Y. and Wang, S., "The identification of coherent structures using proper orthogonal decomposition and dynamic mode decomposition", J*ournal of Fluids and Structure*, Vol. 49 (2014), pp. 53-72.

[7] Aranyi P., Janiga G., Zahringer K. and Thevenin D., "Analysis of different POD methods for PIV measurements in complex unsteady flows", *International Journal of Heat and Fluid Flow*, Vol. 43 (2013), pp. 204-211.

[8] Sirovich L., "Turbulence and the dynamics of coherent structure", *Quarterly of Applied Mathematics*, Vol. 45 (1987), pp. 561-590.

[9] Berkooz G., Holmes S. and Lumley J.L., "The proper orthogonal decomposition in the analysis of turbulent flows", *Annual Review of Fluid Mechanics*, Vol. 25 (1993), pp. 539-575.

[10] Chu C.C. and Chang K.C., "Estimating the energy contribution of coherent structure in a cylindrical near-wake flow using proper orthogonal decomposition", *Journal of Fluid Science and Technology*, Vol. 18 (1), (2023), DOI: 10.1299/jfst.2023jfst0004.

[11] Roshko A., 'Experiments on the flow past a circular cylinder at very high Reynolds number", *Journal of Fluid Mechanics*, Vol. 10 (1961), pp. 345-356.

[12] Chang K.C., Lin T.H. and Chu C.C., "Sensitivity study on POD analysis for near wake behind circular cylinder", Proceedings of 10th Conference on Experimental Heat Transfer, Fluid Mechanics and Thermodynamics, paper no.: 11, Rhode Island, Greece, 22-26, August (2024).

[13] Lin T.H., "Parametric study on POD analysis of near-wake flow behind circular cylinder", M. S. thesis, National Cheng Kung University, Taiwan (2021) (in Chinese).

[14] Dynnikova G.Ya., Dynnikov Ya.A. and Guvernyuk S.V., "Mechanism underlying K*á*rm*á*n vortex street breakdown preceding secondary vortex street formation", *Physics of Fluids*, Vol. 28, No. 5 (2016), 054101.

[15] Yiu M.W., Zhou Y., Zhou T. and Cheng L., "Reynolds number effects on three-dimensional vorticity in a turbulent wake", *AIAA Journal*, Vol. 42, No. 5, (2004) 1009-1016.

[16] Wu J., Shridan J. Welsh M.C. and Hourigan K., "Three-dimensional vortex structures in a cylinder wake", *Journal of Fluid Mechanics*, Vol. 312 (1996), pp. 201-222.

[17] Huang J.F., Zhou Y. and Zhou T., "Three-dimensional wake structure measurement using a modified PIV technique", *Experiments in Fluids*, Vol. 40 (2006), pp. 884-896.